

# Measurement of in-medium jet modification using direct photon+jet and $\pi^0$ +jet correlations in $p + p$ and central Au + Au collisions at $\sqrt{s_{\text{NN}}} = 200$ GeV

The STAR Collaboration

The STAR Collaboration presents measurements of the semi-inclusive distribution of charged-particle jets recoiling from energetic direct-photon ( $\gamma_{\text{dir}}$ ) and neutral-pion ( $\pi^0$ ) triggers in  $p + p$  and central Au + Au collisions at  $\sqrt{s_{\text{NN}}} = 200$  GeV over a broad kinematic range, for jet resolution parameters  $R = 0.2$  and  $0.5$ . Medium-induced jet yield suppression is observed to be larger for  $R = 0.2$  than for  $0.5$ , reflecting the angular range of jet energy redistribution due to quenching. The magnitude of suppression is similar for  $\gamma_{\text{dir}}$ - and  $\pi^0$ -triggered data, which constrains the color-charge and path-length dependence of jet quenching. Theoretical model calculations incorporating jet quenching do not fully describe the measurements.

*Introduction* - Strongly-interacting matter at high energy density and temperature is a state of deconfined quarks and gluons called the Quark-Gluon Plasma [1, 2]. The QGP filled the early universe a few microseconds after the Big Bang, and is recreated today using energetic collisions of heavy atomic nuclei at the Relativistic Heavy Ion Collider (RHIC) and the Large Hadron Collider (LHC) [3, 4].

Jets are correlated sprays of hadrons arising from the fragmentation of energetic quarks and gluons generated in hard partonic interactions (momentum transfer  $Q^2 \gtrsim 1 - 2$  GeV $^2$ ). Calculations based on perturbative quantum chromodynamics (pQCD) agree well with jet measurements in  $p + p$  collisions over a wide kinematic range [5–9]. Jet production is a high- $Q^2$  process, occurring at times  $\Delta\tau \sim 1/Q \ll 1$  fm/c, which is prior to the formation of the QGP in a heavy-ion collision. Jets propagate in the QGP and interact with it (“jet quenching”) [10–13]. These interactions generate several observable effects: suppression in jet yield due to energy loss, modification of internal jet structure, and broadening of angular distributions in coincidence observables due to scattering off QGP constituents. Comparison of measurements and calculations of jet modifications probe the structure and dynamics of the QGP [14, 15].

Reconstructed jet measurements in heavy-ion collisions are challenging, due to the large background from uncorrelated processes [15]. The initial observation of jet quenching was therefore based on inclusive production and correlations of high transverse momentum (high- $p_{\text{T}}$ ) hadrons [16–28]. These measurements have been used to constrain the QGP transport parameter  $\hat{q}$ , which characterizes the momentum transfer between an energetic jet and the QGP [29–31].

High- $p_{\text{T}}$  hadron measurements are sensitive primarily to medium-induced energy loss, however, and reconstructed jet measurements are required for more detailed exploration of the mechanisms underlying jet quenching [32–47]. Of special interest is the correlation between a direct photon and a recoil jet ( $\gamma_{\text{dir}}+\text{jet}$ ); photons are colorless and do not interact significantly with the QGP [48, 49], and therefore provide an unmodified

reference for measuring jet quenching via correlated recoil jets [50]. At leading perturbative order, the dominant channel for  $\gamma_{\text{dir}}+\text{jet}$  production at RHIC energies is QCD Compton scattering,  $qg \rightarrow \gamma q$ , in which the direct photon and the quark jet are balanced in  $p_{\text{T}}$ . While higher-order effects modify this simple picture [51], the  $\gamma_{\text{dir}}+\text{jet}$  coincidence channel remains a promising approach for high-precision measurements and calculations of jet quenching.

Measurements of  $\gamma_{\text{dir}}+\text{jet}$  coincidence observables have been carried out for  $p + p$  and Pb + Pb collisions at the LHC [40, 52–54]. In-medium modification of recoil jets is observed in Pb + Pb collisions, though with medium-induced energy loss that is smaller in magnitude than the in-vacuum momentum imbalance observed in  $p + p$  collisions.  $Z$ -boson+hadron and  $\gamma_{\text{dir}}+\text{hadron}$  measurements have also been reported [55–58]. To date, no  $\gamma_{\text{dir}}$ -triggered correlation measurements with reconstructed jets have been reported at RHIC.

Measurements of high- $p_{\text{T}}$  hadron+jet coincidences are likewise of interest, particularly with high-statistics charged hadrons or  $\pi^0$  triggers that can be measured precisely in the complex environment of a heavy-ion collision [37, 46, 56]. High- $p_{\text{T}}$  hadrons are fragments of jets, and are therefore generated by a different mixture of partonic processes than direct photons. The simultaneous measurement of  $\gamma_{\text{dir}}$  and hadron-triggered correlations, using the same analysis approach, enables the comparison of jet quenching effects in jet populations with different production spectra, different relative quark and gluon contributions, and different in-medium path-length distributions [59].

In this Letter and companion article [59], the STAR Collaboration presents the first measurement of jet quenching using  $\gamma_{\text{dir}}+\text{jet}$  and  $\pi^0+\text{jet}$  correlations in  $p + p$  collisions and central (0–15%) Au + Au collisions at  $\sqrt{s_{\text{NN}}} = 200$  GeV. The analysis utilizes previous developments for  $\gamma_{\text{dir}}/\pi^0$  discrimination [55, 56] and for correction of the complex jet background in central Au + Au collisions using mixed events (ME) [46]. Jets are reconstructed using the anti- $k_{\text{T}}$  algorithm [60] with resolution parameters (jet “radius”)  $R = 0.2$  and  $0.5$ . Semi-

inclusive distributions of charged-particle jets recoiling from  $\gamma_{\text{dir}}$  (transverse energy  $11 < E_{\text{T}}^{\text{trig}} < 20 \text{ GeV}$ ) and  $\pi^0$  triggers ( $11 < p_{\text{T}}^{\text{trig}} < 15 \text{ GeV}/c$ ) are reported (see [59] for the analysis of other trigger kinematics). These measurements are sensitive to energy loss and intra-jet broadening due to jet quenching. This Letter compares the results to theoretical models incorporating jet quenching, and discusses constraints from such comparisons on the physical mechanisms underlying jet quenching.

*Dataset and analysis* - The STAR detector is described in [61]. The  $p + p$  and Au + Au datasets were recorded during the 2009 and 2014 RHIC runs, respectively. Online event selection utilized a trigger based in the STAR Barrel Electromagnetic Calorimeter (BEMC) [62], which required 1) transverse energy ( $E_{\text{T}}$ ) in one calorimeter tower of at least 4.2 GeV in  $p + p$  and 5.9 GeV in Au + Au collisions; and 2) total  $E_{\text{T}}$  deposited in one or two adjacent towers to be greater than 7.44 GeV in both  $p + p$  and Au + Au collisions. Event-selection cuts are applied to suppress pileup and to remove bad runs. After all event selection cuts, the integrated luminosity accepted for the analysis is  $3.9 \text{ nb}^{-1}$  for Au + Au collisions and  $23 \text{ pb}^{-1}$  for  $p + p$  collisions. Offline analysis follows the procedures described in [46, 56].

Centrality in Au + Au collisions is determined using the uncorrected charged-particle multiplicity measured in pseudo-rapidity  $|\eta| < 0.5$ . Central Au + Au collisions in this analysis correspond to the 15% highest-multiplicity events in the Minimum Bias (MB) population.

High- $E_{\text{T}}$  direct-photon and  $\pi^0$  triggers are measured in the BEMC. Observed high- $E_{\text{T}}$  photons arise from several sources: direct production from partonic  $qg \rightarrow \gamma q$  and  $q\bar{q} \rightarrow \gamma g$  processes; fragmentation from quark bremsstrahlung in jet showers [63]; and hadronic decays, primarily of  $\pi^0$  and  $\eta$  mesons. In Au + Au collisions, high- $E_{\text{T}}$  photons may also be generated by jet interactions in the QGP [64]. Among these processes, direct-photon production is of special interest for the study of jet quenching because it best constrains the scattering kinematics. The contributions of decay and fragmentation photons are therefore largely subtracted in the analysis.

Discrimination of high- $p_{\text{T}}$  single-photon BEMC showers from those due to  $\pi^0$  decay is based on the transverse-shower profile (TSP) measured by the Barrel Shower Max Detector (BSMD) [56]. The purity of the  $\pi^0$  TSP cut is greater than 95%. However, the shower population satisfying the single-photon TSP cut contains an admixture of direct, fragmentation, and decay photons; this population is labeled “gamma-rich” ( $\gamma_{\text{rich}}$ ). The  $\gamma_{\text{dir}}$  fraction of the  $\gamma_{\text{rich}}$  population is determined from the correlated rate of charged hadrons with  $p_{\text{T}} > 1.2 \text{ GeV}/c$  that are adjacent in azimuthal angle  $\varphi$  (“near-side”), assuming that direct-photon triggers have zero correlated rate [56]. For central Au + Au collisions the  $\gamma_{\text{dir}}$  purity varies between  $67 \pm 3\%$  and  $84 \pm 4\%$  over the range  $E_{\text{T}}^{\text{trig}} = 9 - 20 \text{ GeV}$ , while for  $p + p$  collisions it varies between  $43 \pm 5\%$  and

$53 \pm 7\%$ . The  $\gamma_{\text{dir}}$  purity is higher in Au + Au than  $p + p$  collisions because of  $\pi^0$  yield suppression due to jet quenching [65]. To obtain the recoil-jet spectrum for  $\gamma_{\text{dir}}$  triggers, the recoil-jet distribution due to background in the  $\gamma_{\text{rich}}$  population (dominated by decay photons) is subtracted assuming its recoil-jet distribution is the same as that of identified  $\pi^0$  triggers.

BEMC showers are then assigned to bins with  $11 < E_{\text{T}}^{\text{trig}} < 15$  and  $15 < E_{\text{T}}^{\text{trig}} < 20 \text{ GeV}$  for  $\gamma_{\text{rich}}$  and  $\pi^0$ -identified triggers. The number of triggers in each bin is tabulated in Ref. [59].

Charged-particle tracks are reconstructed offline using hits in the STAR Time Projection Chamber (TPC) [66]. Jet reconstruction utilizes primary tracks, which include the event vertex in the momentum fit. The acceptance for primary tracks is  $|\eta| < 1.0$  and  $0.2 < p_{\text{T},\text{track}} < 30 \text{ GeV}/c$ , over the full azimuth. The tracking efficiency for primary tracks with  $p_{\text{T},\text{track}} > 2 \text{ GeV}/c$  is 72% in central Au + Au collisions and 82% in  $p + p$  collisions. Primary-track momentum resolution is approximately  $\sigma_{p_{\text{T}}}/p_{\text{T}} = 0.01 \cdot p_{\text{T}}/(\text{GeV}/c)$  in both systems.

Charged-particle jets are reconstructed from primary tracks using the  $k_{\text{T}}$  [67] and anti- $k_{\text{T}}$  [60] algorithms for jet-resolution parameters  $R = 0.2$  and  $0.5$ , with  $E$ -scheme recombination and active ghost area 0.01 [67]. Event-wise estimation of the median energy density  $\rho$  [68] utilizes  $k_{\text{T}}$  jets, with the two hardest jet candidates excluded for Au + Au collisions and the single hardest jet candidate excluded for  $p + p$  collisions. The physics analysis is based on anti- $k_{\text{T}}$  jets. Jet candidates are accepted if their centroid lies within  $|\eta| < 1.0 - R$  and their area satisfies  $A_{\text{jet}} > 0.05$  for  $R = 0.2$  and  $A_{\text{jet}} > 0.65$  for  $R = 0.5$  [46]. The raw  $p_{\text{T}}$  ( $p_{\text{T},\text{jet}}^{\text{raw}}$ ) of accepted jet candidates is adjusted by the event-wise estimated background,  $p_{\text{T},\text{jet}}^{\text{reco},i} = p_{\text{T},\text{jet}}^{\text{raw},i} - \rho A_{\text{jet}}^i$ , where  $i$  labels a jet candidate and  $A_{\text{jet}}^i$  is its area (see Ref. [46] for notation and definitions). The Jet Energy Resolution and the Jet Energy Scale are similar to those in Ref. [46].

Events with a  $\gamma_{\text{rich}}$  or  $\pi^0$  trigger in the defined  $E_{\text{T}}^{\text{trig}}$  bins are selected for the correlation analysis. The recoil-jet azimuthal acceptance is  $\frac{3\pi}{4} < \Delta\varphi < \frac{5\pi}{4}$ , where  $\Delta\varphi$  is the azimuthal separation between the trigger and jet centroid. All jet candidates satisfying this cut are accepted, with no jet-wise discrimination of correlated and uncorrelated yield with respect to the trigger. The trigger-normalized semi-inclusive recoil-jet distribution is then tabulated for all events in each trigger class and collision system. Because event selection is based solely on the presence of a trigger which is distributed like the inclusive production cross section, in the absence of background the trigger-normalized distribution is equivalent to the ratio of perturbatively calculable cross sections [37, 46],

$$\frac{1}{N_{\text{trig}}} \cdot \frac{dN_{\text{jet}}}{dp_{T,\text{jet}}^{\text{ch}}} \Big|_{p_T^{\text{trig}}} = \left( \frac{1}{\sigma^{\text{A+A} \rightarrow \text{trig}}} \cdot \frac{d\sigma^{\text{A+A} \rightarrow \text{trig+jet}}}{dp_{T,\text{jet}}^{\text{ch}}} \right) \Big|_{p_T^{\text{trig}}}, \quad (1)$$

where  $N_{\text{trig}}$  is the number of triggers,  $\frac{dN_{\text{jet}}}{dp_{T,\text{jet}}^{\text{ch}}}$  is the  $p_T$ -differential recoil-jet distribution,  $\sigma^{\text{A+A} \rightarrow \text{trig}}$  is the inclusive production cross section for the trigger, and  $\sigma^{\text{A+A} \rightarrow \text{trig+jet}}$  is the production cross section for trigger and recoil jets in the acceptance.

The reconstructed jet population in central Au + Au collisions includes a large uncorrelated jet yield, which is corrected at the level of the ensemble-averaged distribution by the ME procedure [46]. After subtraction of the uncorrelated jet yield distribution, correction for  $p_T$ -smearing due to instrumental effects and residual background fluctuations is carried out using unfolding [69, 70]. The corrected distribution for  $\gamma_{\text{dir}}$  triggers is determined from the linear combination of  $\gamma_{\text{rich}}$  and  $\pi^0$ -triggered distributions, accounting for the  $\gamma_{\text{dir}}$  purity [56, 59].

The largest systematic uncertainties in central Au + Au collisions arise from the uncorrelated background yield correction; choice of unfolding algorithm, regularization, and prior; response matrix; tracking efficiency; and the  $\gamma_{\text{dir}}$  purity. In  $p + p$  collisions, the largest systematic uncertainties are due to the tracking efficiency, unfolding, and the  $\gamma_{\text{dir}}$  purity. The cumulative uncertainty is the quadrature sum of all uncertainty components, and is shown in all figures as a continuous band to indicate large off-diagonal covariance [46, 47].

The distribution of  $E_T^{\text{trig}}$  is not corrected for the finite energy resolution of the BEMC. The estimated effect of this resolution on the recoil-jet spectrum is approximately 20-40% at high  $p_{T,\text{jet}}^{\text{ch}}$ , depending upon  $E_T^{\text{trig}}$  [59]. Accurate comparison of the measured recoil-jet distributions to theoretical models therefore requires the calculated distributions to be smeared by the resolution function, which is specified in Ref. [59]. However, since the trigger-spectrum shapes in Au + Au and  $p + p$  collisions are similar and the BEMC resolution affects the trigger distributions in Au + Au and  $p + p$  similarly, its effect on recoil-jet distributions largely cancels in their ratio. We therefore do not apply this smearing for the model comparisons below.

The measurements are compared to the following theoretical calculations incorporating jet quenching, which are described briefly in Ref. [59]: Jet-fluid model [71]; Linear Boltzmann Transport (LBT) model [72]; Coupled linear Boltzmann transport and hydro model (CoLBT-hydro) [73, 74]; Soft Collinear Effective Theory (SCET) model [75]; and Hybrid model [76]. A significant difference between the models is their treatment of “back-reaction,” which refers to excitation of the QGP medium due to absorption of energy from the jet-medium interaction. Back-reaction may generate a jet-associated

wake, which in practice is included in the correlated energy of the jet measurement, modifying observed jet  $p_T$  and shape distributions. The jet-fluid and SCET models do not incorporate back-reaction, whereas the LBT, CoLBT, and Hybrid models have different back-reaction implementations (see Ref. [59]). The Hybrid model is optionally run without back-reaction.

*Results* - Corrected recoil-jet distributions are reported for  $p_{T,\text{jet}}^{\text{ch}} > 3 \text{ GeV}/c$ , which is lower than is commonly used in jet measurements. We do not assert that such low values of  $p_{T,\text{jet}}$  are interpretable perturbatively. Rather, our usage of the term “jet” in this context is purely operational, i.e. application of the anti- $k_T$  clustering algorithm to measure trigger-correlated recoil-energy flow within an aperture of radius  $\sim R$ . The phenomenology of these distributions, together with comparison to theoretical calculations, may then elucidate the underlying physical processes, both perturbative and non-perturbative.

Figure 1 shows corrected trigger-normalized semi-inclusive recoil-jet distributions for selected  $E_T^{\text{trig}}$  bins measured in central Au + Au and  $p + p$  collisions, for  $\gamma_{\text{dir}}$  and  $\pi^0$  triggers, and for recoil jets with  $R = 0.2$  and  $0.5$ . Significant yield suppression is observed in central Au + Au relative to  $p + p$  collisions with both triggers for  $R = 0.2$ , while less suppression is observed for  $R = 0.5$ .

Figure 2 shows  $I_{\text{AA}}$ , the ratio of the semi-inclusive recoil-jet yields measured in central Au + Au and  $p + p$  collisions for the same trigger and  $R$ . For  $11 < E_T^{\text{trig}} < 15 \text{ GeV}$ ,  $I_{\text{AA}}$  is consistent within uncertainties for  $\gamma_{\text{dir}}$  and  $\pi^0$  triggers. Yield suppression ( $I_{\text{AA}} < 1$ ) arises from the combined effects of population-averaged energy loss and spectrum shape. Since the recoil-jet spectrum for  $p + p$  collisions is steeper for  $\gamma_{\text{dir}}$  than for  $\pi^0$  triggers in  $11 < E_T^{\text{trig}} < 15 \text{ GeV}$  [59], Fig. 2 may indicate larger average energy loss for the  $\pi^0$ -triggered population. Also shown are the corresponding Hybrid Model calculations, which are likewise consistent for the two triggers. Such comparisons can elucidate the roles of relative quark/gluon content, path-length distribution, and energy-loss fluctuations [77] in generating medium-induced energy loss.

Marked recoil-yield suppression is observed in central Au + Au collisions for  $R = 0.2$ , with reduced suppression for  $R = 0.5$ , for both triggers in  $11 < E_T^{\text{trig}} < 15 \text{ GeV}$  and for  $\gamma_{\text{dir}}$  triggers in  $15 < E_T^{\text{trig}} < 20 \text{ GeV}$ . Taking into account the spectrum shapes in Fig. 1, larger suppression for  $R = 0.2$  than for 0.5 corresponds to smaller energy loss for  $R = 0.5$ ; qualitatively, a larger fraction of the initial jet energy is captured in a cone of opening 0.5 than 0.2 radians. This provides a new measurement of the angular scale over which jet energy is redistributed by quenching.

For recoil jets with  $R = 0.2$ , the model calculations are similar for  $\pi^0$  and  $\gamma_{\text{dir}}$  triggers in  $11 < E_T^{\text{trig}} < 15 \text{ GeV}$  and agree with the data within uncertainties, while for  $\gamma_{\text{dir}}$  triggers in  $15 < E_T^{\text{trig}} < 20 \text{ GeV}$ , less suppression

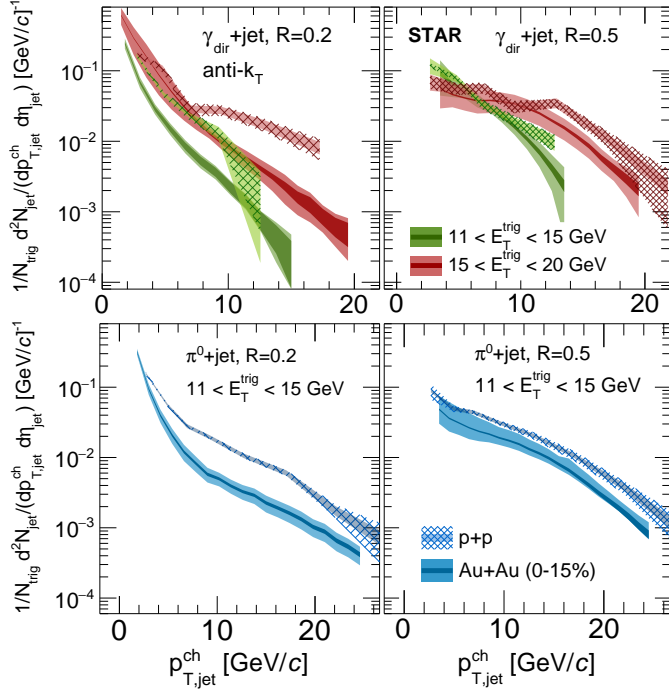


FIG. 1. (Color online) Corrected semi-inclusive distributions of charged-particle jets recoiling from  $\gamma_{\text{dir}}$  (upper) and  $\pi^0$  (lower) triggers measured in central  $\text{Au} + \text{Au}$  and  $p + p$  collisions at  $\sqrt{s_{\text{NN}}} = 200 \text{ GeV}$ , for  $R = 0.2$  (left) and  $0.5$  (right). Dark bands show statistical error; light bands ( $\text{Au} + \text{Au}$ ) or hashed bands ( $p + p$ ) show systematic uncertainty.

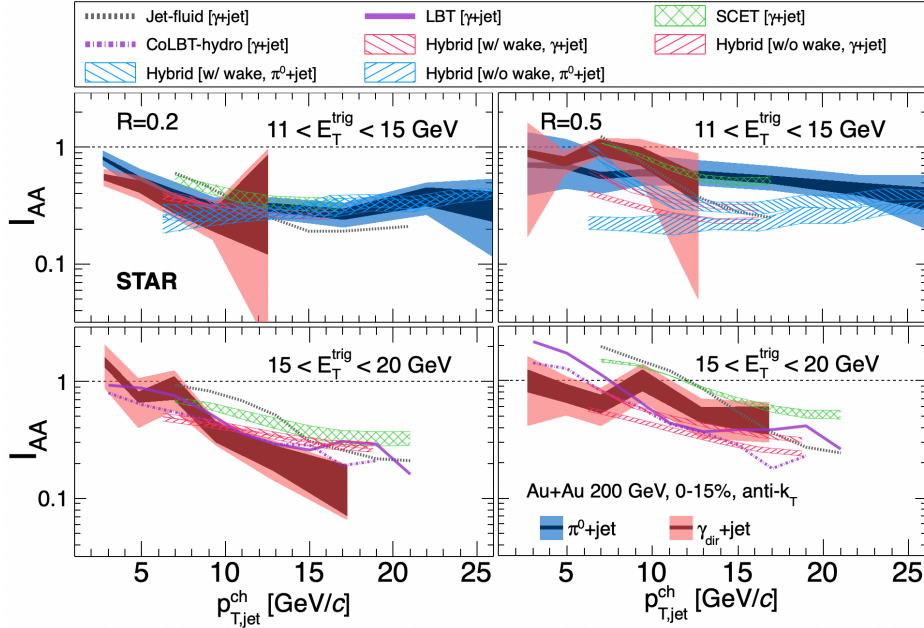


FIG. 2. (Color online) Ratio of recoil-jet yields in central  $\text{Au} + \text{Au}$  and  $p + p$  collisions ( $I_{\text{AA}}$  [59]) at  $\sqrt{s_{\text{NN}}} = 200 \text{ GeV}$  shown in Fig. 1. Uncertainty bands account for correlated uncertainties in numerator and denominator. Theoretical calculations are described in text.

is predicted than observed in data. For  $R = 0.5$ , some of the models reproduce qualitatively the reduced suppression observed for both triggers, but none agrees well

with the data within uncertainties. The Hybrid model calculations with and without wake are similar for this observable. Overall, the agreement of models and data

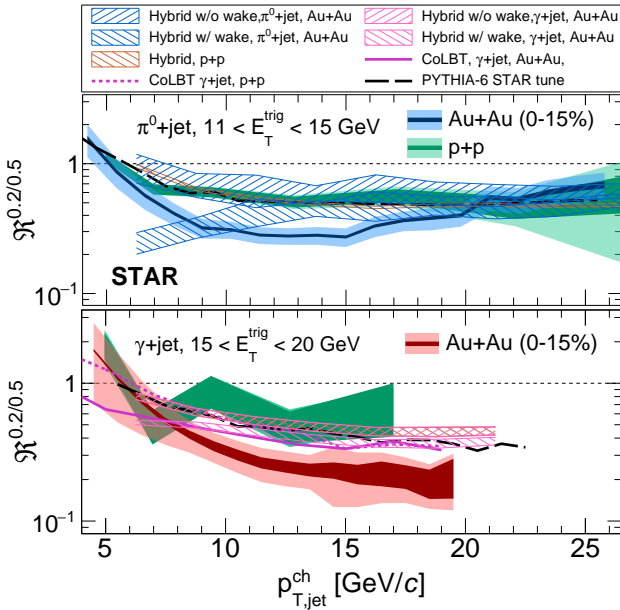


FIG. 3. (Color online) Ratio of recoil-jet yields with  $R = 0.2$  and  $0.5$ ,  $\mathfrak{R}^{0.2/0.5}$  [59] in central  $Au+Au$  and  $p+p$  collisions for  $\pi^0$  triggers with  $11 < E_T^{trig} < 15$  GeV (upper) and  $\gamma_{dir}$  triggers with  $15 < E_T^{trig} < 20$  GeV (lower). Uncertainty bands account for correlated uncertainties in numerator and denominator. Theoretical calculations are described in text.

in Fig. 2 is limited, with no clear discrimination of the models.

Figure 3 shows  $\mathfrak{R}^{0.2/0.5}$ , the ratio of recoil-jet yields for  $R = 0.2$  and  $0.5$  separately in  $p+p$  and  $Au+Au$  collisions, which probes intra-jet broadening [59]. The  $p+p$  collision distributions are well-described by PYTHIA-6 STAR tune [78, 79]. Similar measurements by the ALICE Collaboration at the LHC are likewise well-described by PYTHIA [37] (see Ref. [59] for further discussion).

Significant suppression of  $\mathfrak{R}^{0.2/0.5}$  is observed for central  $Au+Au$  compared to  $p+p$  collisions, in contrast to the ALICE measurement [37]. For example, for  $\pi^0$  triggers with  $11 < E_T^{trig} < 15$  GeV the value of  $\mathfrak{R}^{0.2/0.5}$  in the range  $10 < p_{T,jet}^{ch} < 15$   $GeV/c$  is  $0.26 \pm 0.09$  (sys) for  $Au+Au$  and  $0.50 \pm 0.06$  (sys) for  $p+p$  collisions, with the statistical error smaller than the systematic uncertainty. This is clear evidence of intra-jet broadening due to jet quenching. Intra-jet broadening has also been studied using other observables (e.g. Ref. [80, 81]).

Back-reaction generates a jet-associated wake, which broadens the jet transverse energy profile. The models considered here have different implementations of back-reaction, or do not include back-reaction. However, all models predict a similar value of  $\mathfrak{R}^{0.2/0.5}$  in  $Au+Au$  and  $p+p$  collisions, in contrast to the observed larger suppression in  $Au+Au$  collisions. None of the models reproduces the magnitude of intra-jet broadening observed in data.

**Summary-** This paper presents the first measurement at RHIC of jet quenching utilizing the coincidence of  $\gamma_{dir}$  and  $\pi^0$  triggers with reconstructed jets in central  $Au+Au$  and in  $p+p$  collisions. Comparison of recoil-jet yields in  $Au+Au$  and  $p+p$  collisions ( $I_{AA}$ ) shows significant medium-induced yield suppression, with greater suppression observed for  $R = 0.2$  than for  $0.5$ . The yield ratio for  $R = 0.2$  and  $0.5$ ,  $\mathfrak{R}^{0.2/0.5}$ , likewise exhibits greater suppression for  $Au+Au$  than  $p+p$  collisions.

These observations are evidence of significant medium-induced intra-jet broadening at angular scales less than  $0.5$  radians. The comparison of  $\gamma_{dir}$  and  $\pi^0$ -triggered distributions probes the relative contributions to jet quenching of quark/gluon fraction, path length, and density fluctuations. Theoretical calculations incorporating jet quenching do not describe the full set of reported data within uncertainties, in particular exhibiting weaker intra-jet broadening than observed.

**Acknowledgments-** We thank Shanshan Cao, Tan Luo, Guang-You Qin, Abhijit Majumder, Daniel Pablos, Krishna Rajagopal, Chathuranga Sirimanna, Xin-Nian Wang, and Ivan Vitev for providing theoretical calculations. We thank the RHIC Operations Group and RCF at BNL, the NERSC Center at LBNL, and the Open Science Grid consortium for providing resources and support. This work was supported in part by the Office of Nuclear Physics within the U.S. DOE Office of Science, the U.S. National Science Foundation, National Natural Science Foundation of China, Chinese Academy of Science, the Ministry of Science and Technology of China and the Chinese Ministry of Education, the Higher Education Sprout Project by Ministry of Education at NCKU, the National Research Foundation of Korea, Czech Science Foundation and Ministry of Education, Youth and Sports of the Czech Republic, Hungarian National Research, Development and Innovation Office, New National Excellency Programme of the Hungarian Ministry of Human Capacities, Department of Atomic Energy and Department of Science and Technology of the Government of India, the National Science Centre and WUT ID-UB of Poland, the Ministry of Science, Education and Sports of the Republic of Croatia, German Bundesministerium für Bildung, Wissenschaft, Forschung und Technologie (BMBF), Helmholtz Association, Ministry of Education, Culture, Sports, Science, and Technology (MEXT) and Japan Society for the Promotion of Science (JSPS).

- 
- [1] J. C. Collins and M. J. Perry, Phys. Rev. Lett. **34**, 1353 (1975).
  - [2] E. V. Shuryak, Sov. Phys. JETP **47**, 212 (1978).
  - [3] W. Busza, K. Rajagopal, and W. van der Schee, Ann. Rev. Nucl. Part. Sci. **68**, 339 (2018), arXiv:1802.04801 [hep-ph].

- [4] J. W. Harris and B. Müller, (2023), arXiv:2308.05743 [hep-ph].
- [5] B. I. Abelev et al. (STAR), Phys. Rev. Lett. **97**, 252001 (2006), arXiv:hep-ex/0608030.
- [6] L. Adamczyk et al. (STAR), Phys. Rev. D **95**, 071103 (2017), arXiv:1610.06616 [hep-ex].
- [7] B. Abelev et al. (ALICE), Phys. Lett. B **722**, 262 (2013), arXiv:1301.3475 [nucl-ex].
- [8] G. Aad et al. (ATLAS), JHEP **02**, 153 (2015), [Erratum: JHEP **09**, 141 (2015)], arXiv:1410.8857 [hep-ex].
- [9] V. Khachatryan et al. (CMS), JHEP **03**, 156 (2017), arXiv:1609.05331 [hep-ex].
- [10] J. D. Bjorken, “Energy Loss of Energetic Partons in Quark - Gluon Plasma: Possible Extinction of High  $p_T$  Jets in Hadron - Hadron Collisions,” (1982).
- [11] X.-N. Wang, M. Gyulassy, and M. Plumer, Phys. Rev. D **51**, 3436 (1995), arXiv:hep-ph/9408344.
- [12] R. Baier, Y. L. Dokshitzer, A. H. Mueller, and D. Schiff, Phys. Rev. C **58**, 1706 (1998), arXiv:hep-ph/9803473.
- [13] M. Gyulassy, P. Levai, and I. Vitev, Phys. Rev. Lett. **85**, 5535 (2000), arXiv:nucl-th/0005032.
- [14] A. Majumder and M. Van Leeuwen, Prog. Part. Nucl. Phys. **66**, 41 (2011), arXiv:1002.2206 [hep-ph].
- [15] L. Cunqueiro and A. M. Sickles, Prog. Part. Nucl. Phys. **124**, 103940 (2022), arXiv:2110.14490 [nucl-ex].
- [16] C. Adler et al. (STAR), Phys. Rev. Lett. **89**, 202301 (2002), arXiv:nucl-ex/0206011.
- [17] C. Adler et al. (STAR), Phys. Rev. Lett. **90**, 082302 (2003), arXiv:nucl-ex/0210033.
- [18] J. Adams et al. (STAR), Phys. Rev. Lett. **91**, 172302 (2003), arXiv:nucl-ex/0305015.
- [19] J. Adams et al. (STAR), Phys. Rev. Lett. **97**, 162301 (2006), arXiv:nucl-ex/0604018.
- [20] L. Adamczyk et al. (STAR), Phys. Rev. Lett. **112**, 122301 (2014), arXiv:1302.6184 [nucl-ex].
- [21] K. Adcox et al. (PHENIX), Phys. Rev. Lett. **88**, 022301 (2002), arXiv:nucl-ex/0109003.
- [22] A. Adare et al. (PHENIX), Phys. Rev. C **87**, 034911 (2013), arXiv:1208.2254 [nucl-ex].
- [23] A. Adare et al. (PHENIX), Phys. Rev. Lett. **104**, 252301 (2010), arXiv:1002.1077 [nucl-ex].
- [24] K. Aamodt et al. (ALICE), Phys. Rev. Lett. **108**, 092301 (2012), arXiv:1110.0121 [nucl-ex].
- [25] B. Abelev et al. (ALICE), Phys. Lett. B **720**, 52 (2013), arXiv:1208.2711 [hep-ex].
- [26] J. Adam et al. (ALICE), Phys. Lett. B **763**, 238 (2016), arXiv:1608.07201 [nucl-ex].
- [27] S. Chatrchyan et al. (CMS), Eur. Phys. J. C **72**, 1945 (2012), arXiv:1202.2554 [nucl-ex].
- [28] S. Chatrchyan et al. (CMS), Eur. Phys. J. C **72**, 2012 (2012), arXiv:1201.3158 [nucl-ex].
- [29] N. Armesto, M. Cacciari, T. Hirano, J. L. Nagle, and C. A. Salgado, J. Phys. G **37**, 025104 (2010), arXiv:0907.0667 [hep-ph].
- [30] K. M. Burke et al. (JET), Phys. Rev. C **90**, 014909 (2014), arXiv:1312.5003 [nucl-th].
- [31] S. Cao et al. (JETSCAPE), Phys. Rev. C **104**, 024905 (2021), arXiv:2102.11337 [nucl-th].
- [32] B. Abelev et al. (ALICE), JHEP **03**, 013 (2014), arXiv:1311.0633 [nucl-ex].
- [33] J. Adam et al. (ALICE), Phys. Lett. B **746**, 1 (2015), arXiv:1502.01689 [nucl-ex].
- [34] S. Acharya et al. (ALICE), Phys. Rev. C **101**, 034911 (2020), arXiv:1909.09718 [nucl-ex].
- [35] G. Aad et al. (ATLAS), Phys. Rev. Lett. **114**, 072302 (2015), arXiv:1411.2357 [hep-ex].
- [36] V. Khachatryan et al. (CMS), Phys. Rev. C **96**, 015202 (2017), arXiv:1609.05383 [nucl-ex].
- [37] J. Adam et al. (ALICE), JHEP **09**, 170 (2015), arXiv:1506.03984 [nucl-ex].
- [38] G. Aad et al. (ATLAS), Phys. Rev. Lett. **105**, 252303 (2010), arXiv:1011.6182 [hep-ex].
- [39] S. Chatrchyan et al. (CMS), Phys. Lett. B **712**, 176 (2012), arXiv:1202.5022 [nucl-ex].
- [40] S. Chatrchyan et al. (CMS), Phys. Lett. B **718**, 773 (2013), arXiv:1205.0206 [nucl-ex].
- [41] A. M. Sirunyan et al. (CMS), Phys. Rev. Lett. **121**, 242301 (2018), arXiv:1801.04895 [hep-ex].
- [42] S. Acharya et al. (ALICE), Phys. Lett. B **776**, 249 (2018), arXiv:1702.00804 [nucl-ex].
- [43] S. Acharya et al. (ALICE), Phys. Lett. B **802**, 135227 (2020), arXiv:1905.02512 [nucl-ex].
- [44] A. M. Sirunyan et al. (CMS), Phys. Rev. Lett. **120**, 142302 (2018), arXiv:1708.09429 [nucl-ex].
- [45] L. Adamczyk et al. (STAR), Phys. Rev. Lett. **119**, 062301 (2017), arXiv:1609.03878 [nucl-ex].
- [46] L. Adamczyk et al. (STAR), Phys. Rev. C **96**, 024905 (2017), arXiv:1702.01108 [nucl-ex].
- [47] J. Adam et al. (STAR), Phys. Rev. C **102**, 054913 (2020), arXiv:2006.00582 [nucl-ex].
- [48] S. Afanasiev et al. (PHENIX), Phys. Rev. Lett. **109**, 152302 (2012), arXiv:1205.5759 [nucl-ex].
- [49] A. M. Sirunyan et al. (CMS), JHEP **07**, 116 (2020), arXiv:2003.12797 [hep-ex].
- [50] X.-N. Wang, Z. Huang, and I. Sarcevic, Phys. Rev. Lett. **77**, 231 (1996), arXiv:hep-ph/9605213 [hep-ph].
- [51] W. Dai, I. Vitev, and B.-W. Zhang, Phys. Rev. Lett. **110**, 142001 (2013), arXiv:1207.5177 [hep-ph].
- [52] A. M. Sirunyan et al. (CMS), Phys. Lett. B **785**, 14 (2018), arXiv:1711.09738 [nucl-ex].
- [53] M. Aaboud et al. (ATLAS), Phys. Lett. B **789**, 167 (2019), arXiv:1809.07280 [nucl-ex].
- [54] G. Aad et al. (ATLAS), (2023), arXiv:2303.10090 [nucl-ex].
- [55] B. I. Abelev et al. (STAR), Phys. Rev. C **82**, 034909 (2010), arXiv:0912.1871 [nucl-ex].
- [56] L. Adamczyk et al. (STAR), Phys. Lett. B **760**, 689 (2016), arXiv:1604.01117 [nucl-ex].
- [57] Ü. Acharya et al. (PHENIX), Phys. Rev. C **102**, 054910 (2020), arXiv:2005.14270 [hep-ex].
- [58] G. Aad et al. (ATLAS), Phys. Rev. Lett. **126**, 072301 (2021), arXiv:2008.09811 [nucl-ex].
- [59] (2023), arXiv:2309.00145 [nucl-ex].
- [60] M. Cacciari, G. P. Salam, and G. Soyez, JHEP **04**, 063 (2008), arXiv:0802.1189 [hep-ph].
- [61] K. H. Ackermann et al. (STAR), Nucl. Instrum. Meth. A **499**, 624 (2003).
- [62] M. Beddo et al. (STAR), Nucl. Instrum. Meth. A **499**, 725 (2003).
- [63] J. F. Owens, Rev. Mod. Phys. **59**, 465 (1987).
- [64] R. J. Fries, B. Muller, and D. K. Srivastava, Phys. Rev. Lett. **90**, 132301 (2003), arXiv:nucl-th/0208001.
- [65] S. S. Adler et al. (PHENIX), Phys. Rev. Lett. **94**, 232301 (2005), arXiv:nucl-ex/0503003.
- [66] M. Anderson et al., Nucl. Instrum. Meth. A **499**, 659 (2003), arXiv:nucl-ex/0301015 [nucl-ex].
- [67] M. Cacciari, G. P. Salam, and G. Soyez, Eur. Phys. J. C **72**, 1896 (2012), arXiv:1111.6097 [hep-ph].

- [68] M. Cacciari and G. P. Salam, Phys. Lett. **B** **659**, 119 (2008), arXiv:0707.1378 [hep-ph].
- [69] A. Hocker and V. Kartvelishvili, Nucl. Instrum. Meth. **A** **372**, 469 (1996), arXiv:hep-ph/9509307 [hep-ph].
- [70] G. D'Agostini, Nucl. Instrum. Meth. **A** **362**, 487 (1995).
- [71] N.-B. Chang and G.-Y. Qin, Phys. Rev. C **94**, 024902 (2016), arXiv:1603.01920 [hep-ph].
- [72] T. Luo, S. Cao, Y. He, and X.-N. Wang, Phys. Lett. B **782**, 707 (2018), arXiv:1803.06785 [hep-ph].
- [73] W. Zhao, W. Ke, W. Chen, T. Luo, and X.-N. Wang, Phys. Rev. Lett. **128**, 022302 (2022), arXiv:2103.14657 [hep-ph].
- [74] W. Chen, S. Cao, T. Luo, L.-G. Pang, and X.-N. Wang, Phys. Lett. B **777**, 86 (2018), arXiv:1704.03648 [nucl-th].
- [75] M. D. Sievert, I. Vitev, and B. Yoon, Phys. Lett. B **795**, 502 (2019), arXiv:1903.06170 [hep-ph].
- [76] J. Casalderrey-Solana, Z. Hulcher, G. Milhano, D. Pablos, and K. Rajagopal, Phys. Rev. C **99**, 051901 (2019), arXiv:1808.07386 [hep-ph].
- [77] J. G. Milhano and K. C. Zapp, Eur. Phys. J. C **76**, 288 (2016), arXiv:1512.08107 [hep-ph].
- [78] T. Sjostrand, S. Mrenna, and P. Z. Skands, JHEP **05**, 026 (2006), arXiv:hep-ph/0603175.
- [79] J. Adam et al. (STAR), Phys. Rev. D **100**, 052005 (2019), arXiv:1906.02740 [hep-ex].
- [80] L. Adamczyk et al. (STAR), Phys. Rev. Lett. **119**, 062301 (2017), arXiv:1609.03878 [nucl-ex].
- [81] A. M. Sirunyan et al. (CMS), Phys. Rev. Lett. **122**, 152001 (2019), arXiv:1809.08602 [hep-ex].